

# Soft Matter

Accepted Manuscript



This is an *Accepted Manuscript*, which has been through the Royal Society of Chemistry peer review process and has been accepted for publication.

*Accepted Manuscripts* are published online shortly after acceptance, before technical editing, formatting and proof reading. Using this free service, authors can make their results available to the community, in citable form, before we publish the edited article. We will replace this *Accepted Manuscript* with the edited and formatted *Advance Article* as soon as it is available.

You can find more information about *Accepted Manuscripts* in the [Information for Authors](#).

Please note that technical editing may introduce minor changes to the text and/or graphics, which may alter content. The journal's standard [Terms & Conditions](#) and the [Ethical guidelines](#) still apply. In no event shall the Royal Society of Chemistry be held responsible for any errors or omissions in this *Accepted Manuscript* or any consequences arising from the use of any information it contains.

**Measurement of Membrane Tension of Free Standing Lipid Bilayers via  
Laser-Induced Surface Deformation Spectroscopy**

Tomohiko Takei,<sup>1</sup> Tatsuya Yaguchi,<sup>1</sup> Takuya Fujii,<sup>1</sup> Tomonori Nomoto,<sup>1</sup> Taro Toyota,<sup>2</sup>  
and Masanori Fujinami<sup>1\*</sup>

<sup>1</sup> *Department of Applied Chemistry and Biotechnology, Chiba University, 1-33 Yayoi,  
Inage, Chiba 263-8522, Japan*

<sup>2</sup> *Department of Basic Science, The University of Tokyo, 3-8-1 Komaba, Meguro, Tokyo  
153-8902, Japan*

\* Corresponding author:

E-mail: fujinami@faculty.chiba-u.jp

**ABSTRACT**

Non-invasive measurement of membrane tension of free-standing black lipid membranes (BLMs), with sensitivity in the order of  $\mu\text{N}\cdot\text{m}^{-1}$ , was achieved using laser-induced surface deformation (LISD) spectroscopy. The BLM was vertically formed via the folding method and aqueous phases with different refractive indices were added on each side in order to induce radiation pressure by a laser beam. The dynamic response of the deformed BLMs was measured under the periodic intensity modulation and their tensions could be estimated. The dependence of membrane tension on the cholesterol concentration of BLMs composed of phosphatidylcholine and phosphatidylethanolamine was investigated, with the membrane tension increasing from  $1.3 \mu\text{N}\cdot\text{m}^{-1}$  to  $68.1 \mu\text{N}\cdot\text{m}^{-1}$  when the cholesterol concentration increased from zero to 33%. These tension values are much smaller than some of those previously reported, because this method does not suppress membrane fluctuation unlike other conventional methods. Our LISD system can be a promising tool for the measurement of membrane tension in BLMs.

## INTRODUCTION

Cell membranes consist of a continuous double layer of lipid molecules, commonly called lipid bilayer, with a thickness of 4–5 nm and with other molecules embedded in it such as steroids, carotenoids, and membrane proteins. Many different phenomena such as selective ion permeation,<sup>1</sup> membrane fusion,<sup>2</sup> exocytosis, or endocytosis occur at the membranes of living cells.<sup>3</sup> Membrane fluctuations, even including the thermally induced flickering motions, are correlated with several physical properties such as membrane tension, shear elastic modulus, and bending elastic constant, and are often expected to play important roles in reactions and phenomena occurring at cell membranes.<sup>4–7</sup> Hence, many investigations on the physical properties of cell membranes have focused on quantitatively clarifying the relation between membrane fluctuations and membrane physical properties.

In previous studies, mechanical properties of cell membranes have been investigated by using invasive methods<sup>8</sup> such as membrane deformation in the micropipette aspiration technique<sup>9,10</sup>, addition of particle probes controlled by optical tweezers,<sup>11</sup> and tip contact in atomic force microscopy.<sup>12,13</sup> Large membrane deformation by these invasive measurements suppresses membrane fluctuations. Park *et al.*<sup>14</sup> optically measured an  $18\text{--}20 \mu\text{N}\cdot\text{m}^{-1}$  area compression modulus on red blood cells

by using diffraction phase microscopy. They found that their results were lower than a previous reported value of  $300\text{--}500\text{ mN}\cdot\text{m}^{-1}$  obtained by the conventional micropipette aspiration technique.<sup>15</sup> The authors discussed that the difference was probably caused by the strong strain stiffening in the membrane due to the applied pressure during the micropipette aspiration, which resulted in the removal of membrane fluctuations. In order to avoid such suppressions in invasive methods, a noncontact technique using an optical method would be ideal to study the mechanical properties of membranes.

Laser-induced surface deformation (LISD) spectroscopy, developed by Sakai *et al.*,<sup>16</sup> is a non-invasive optical method for measuring surface tension or viscosity through the detection of surface deformation induced by radiation pressure. The interfacial tensions of air-liquid and liquid-liquid interfaces have been determined to be in the range from  $1\text{ }\mu\text{N}\cdot\text{m}^{-1}$  to  $100\text{ mN}\cdot\text{m}^{-1}$ .<sup>17,18</sup> Surface tension of a high-viscosity liquid<sup>19</sup> and the change in surface tension at sol-gel transition<sup>20</sup> have also been reported, but, to the best of our knowledge, the application of LISD method to a lipid bilayer has never been performed.

LISD technique is applicable to an interface having two liquid phases with optically different properties in order to cause radiation pressure at the interface under pump laser irradiation. This deformed interface works like an optical lens, so that

another probe laser beam can be deflected after transmitting the interface, and the intensity of the restricted area in the probe beam is proportional to the inclination of the interface gradient. The response of the deformed interface is dominated by the propagating and dumping waves with different wave numbers. Therefore, the frequency spectrum of the interfacial deformation, or the signal of the probe beam, is obtained by modulating the intensity of the pump laser beam and the interfacial tension can be derived from the characteristic frequency,  $f_c$ , which gives a half of the signal intensity when compared with one at sufficiently low frequency. LISD technique can be used to measure the membrane tension of a lipid bilayer if it can be formed at the interface between two kinds of liquid phases. According to the above-mentioned principle of LISD, light absorption in the system results in a thermal lens effect, which leads to large background noise and disturbs the measurement of pure interfacial displacement due to the radiation pressure. Therefore, the thermal lens effect restricts the application of LISD technique to the living cell, in which a huge amount of substances are involved, and it requires the combination with artificial cell membranes, which are fabricated under chemically controlled condition.

Artificial cell membrane models composed of a continuous lipid bilayer have been widely studied,<sup>21</sup> such as supported lipid membranes,<sup>11,22</sup> tethered membranes,<sup>23</sup>

vesicles,<sup>9,24,25</sup> and droplet interface bilayer (DIB) formed from a liquid droplet.<sup>26,27</sup> One of the candidates for LISD technique is the planar unsupported (freestanding) lipid bilayer membrane,<sup>28–34</sup> which is also known as black film or black lipid membrane (BLM). A BLM becomes a stable barrier between two liquid phases. Since the control of the chemical composition of aqueous phases is easier in BLMs than in vesicles, they have been often used to study ion-channel proteins in membranes. The deformation of BLMs by laser irradiation is determined by radiation pressure and Laplace pressure. The Laplace pressure on the lipid bilayer is caused by its membrane tension.<sup>35</sup> Therefore, it is expected that the LISD spectra obtained can be correlated with the membrane tension of the BLMs.

In this study, we have aimed to achieve the LISD technique for measuring the membrane tension of free-standing lipid bilayers, or BLMs, and investigate its dependence on cholesterol concentration. Cholesterol is one of the main components in cell membranes,<sup>36</sup> with 35% cholesterol being present in eukaryote cells.<sup>37</sup> It is known that cholesterol stabilizes and hardens a membrane composed of phospholipid molecules and that the tension of a lecithin membrane increases with cholesterol concentration.<sup>38</sup> However, since the technique in the previous study<sup>38</sup> monitored the membrane deformation by water pressurization, which could affect fluctuations, a

measurement using non-invasive manner is desired for studying the effect of cholesterol in the mechanical properties and fluctuations of BLMs.

## EXPERIMENTAL SECTION

**Reagents.** L- $\alpha$ -phosphatidylcholine (PC) ( $100 \text{ mg}\cdot\text{mL}^{-1}$  in chloroform solution, Sigma-Aldrich, USA), L- $\alpha$ -phosphatidylethanolamine (PE) ( $10 \text{ mg}\cdot\text{mL}^{-1}$  in chloroform solution, Sigma-Aldrich, USA) were purchased as components for BLMs. Cholesterol was purchased from Kanto Chemical (Japan) and used after recrystallizing three times in methanol. Potassium chloride and HEPES were obtained from Wako Chemical (Japan) and Calbiochem (USA), respectively. Potassium hydroxide, *n*-hexadecane, 1-hexanol, chloroform, ethanol, sucrose, and glucose were purchased from Kanto Chemical. Water was purified using Milli-Q Integral 3 from Millipore (Japan).

In order to mix the phospholipids and cholesterol uniformly, we added the chloroform solution of cholesterol ( $1 \text{ mg}\cdot\text{mL}^{-1}$ ) to that of a mixture ( $34 \mu\text{L}$ ) of PC ( $4.11 \text{ mg}\cdot\text{mL}^{-1}$ ) and PE ( $0.59 \text{ mg}\cdot\text{mL}^{-1}$ ). The mixed chloroform solution in a glass tube was dried under a nitrogen flow affording a thin film. A mixed organic solvent of chloroform, which was purified by an activated aluminum oxide column, and hexane (1:1, v/v) was added to the thin film to adjust the final total concentration of the lipids and cholesterol



to  $2 \text{ mg}\cdot\text{mL}^{-1}$ . The aqueous solutions of glucose and sucrose at a concentration of  $1.5 \text{ mol}\cdot\text{L}^{-1}$  of sugar were prepared in  $1 \text{ mol}\cdot\text{L}^{-1}$  KCl and  $10 \text{ mmol}\cdot\text{L}^{-1}$  HEPES/KOH buffer (pH 7.4)

**Fabrication of BLMs using the Folding Method.** The BLMs were formed vertically using the folding method.<sup>29-34</sup> In this method, a lipid bilayer is formed by folding up two monolayers simultaneously, which spreads on the water surface, so that the organic solvent involved in BLMs becomes much less when compared with other methods such as the “painting” method or the DIB method. As shown in Fig. 1, we designed a PTFE chamber with two 2.0 mL compartments separated by a PTFE film (with  $20 \text{ }\mu\text{m}$  of thickness) with a  $400\text{-}\mu\text{m}$  hole, where the BLM formed. Two fused silica windows with  $\phi 10 \text{ mm}$  sealed with Viton O-rings were attached on each opposite side of the PTFE film so that the laser beams were irradiated and transmitted to and from the BLM in LISD measurements. It is very important to exchange the aqueous solution in the folding method. A syringe (SS-01T, Terumo, Japan) was connected to each compartment with Viton tubes in order to add and remove the aqueous solution. The chamber was cleaned with Milli-Q water and then ethanol in an ultrasonic cleaner for 30 min, just before use. After the ultrasonic cleaning and rinsing with chloroform, the chamber was assembled, and the PTFE film was precoated with a thin layer of

n-hexadecane by adding (dropwise) a 30- $\mu$ L aliquot of 1 wt% n-hexadecane solution in chloroform. Glucose and sucrose solutions (2 mL each) were added to each compartment until the surfaces of the aqueous phases were below the hole. A 110–150  $\mu$ L portion of a lipid solution (PC, PE and/or cholesterol dissolved in chloroform) was spread on each aqueous solution, and the lipid monolayer was formed through vaporization of chloroform. The BLMs were formed by adding aqueous solution gradually in each compartment simultaneously until it covered the hole.

The successful formation of BLMs was evaluated by measuring the capacitance between the two aqueous phases by using a LCR meter (ZM2353, NF Corporation, Japan) by applying 50 mV voltage with 1 kHz frequency. Silver wires coated with AgCl were used as electrodes and were introduced into the compartments.

**Experimental Setup of LISD Technique.** The optical setup for the LISD measurement is schematically shown in Fig. 2. The molar absorption coefficient of water should be as small as possible in order to minimize the thermal lens effect. It was reported that the extinction coefficient of water showed a minimum around 475 nm.<sup>39</sup> Therefore, a 532 nm green laser is one of the most appropriate pump lasers, and a Nd:YVO<sub>4</sub> laser (Excelsior 532 Single Mode, Spectra Physics, USA) with 300 mW was adopted. We measured the dynamic response of the deformed interface under the

periodic modulation in intensity of the pump laser. The pump laser modulated by an acousto-optic modulator (AOM) (AOMO 3080-125, Crystal Technology, Inc., USA) was focused by an objective (M Plan Apo  $\times 10$ , Mitutoyo Corp., Japan) onto the vertically formed BLMs. For monitoring laser spot size, a beam sampler was inserted near the objective, and the laser spot image reflected by the BLMs was focused on a CMOS camera (UI-1640LE-C-HQ, Imaging Development Systems GmbH, Germany) by an achromatic lens ( $f = 120$  mm). A 633-nm red helium-neon laser (05 LHR 171, Melles Griot, USA) with 7 mW was used as a probe laser and focused onto the BLMs coaxially with the pump laser to detect the interface displacement through the interface gradient. The diameter of the probe laser beam was expanded by a  $\times 10$  beam expander (09 LBM 013, Melles Griot, USA) and a smaller beam spot could be obtained compared with that of the pump laser at the focal point. When the pump laser was irradiated, the radiation pressure induced by aqueous phases with different optical properties deformed the BLMs. The probe laser transmitted through the BLMs was collimated by another objective (M Plan Apo  $\times 5$ , Mitutoyo Corp., Japan) and spectrally separated from the pump laser by band-pass filters and a grating. Furthermore, it was focused and detected by a Si PIN photodiode (ET-2030, Electro-Optics Technology, Inc., USA) with a detection area of 100  $\mu\text{m}$  diameter, connected to a current amplifier (DHPCA-100,

FEMTO Messtechnik, Germany). The deformed BLMs between two media with different refractive indices work as an optical lens. Therefore, only when the pump laser modulated with AOM was irradiated to the BLMs, the probe laser deflected was detected.

The signal intensity of the probe laser was analyzed by a lock-in amplifier (SR830, Stanford Research Systems, USA), whose reference was given by the modulation signal of AOM. The modulation frequency was scanned from 100 Hz to 100 kHz and the frequency response spectra of the BLMs were obtained.

When a laser beam with periodic intensity modulation is focused on the BLM, a convex deformation, which is dependent on laser intensity distribution, and the resultant propagating waves are induced on the BLM. Because the finest structure of the deformation is limited by the pump beam diameter,  $2w$ , the excitable half-wavelength of the propagating waves is expected to be longer than  $2w$ . The wave number of the excited propagating wave is similarly restricted to  $\pi/2w$ . Thus, the amplitude of laser-induced deformation is decreased at frequencies higher than the characteristic frequency,  $f_c$ . According to the dispersion relation, assuming wave number  $\pi/2w$  at frequency  $f_c$ ,<sup>17,18</sup> the relation between  $f_c$  and interfacial (BLM membrane) tension,  $\gamma$ , is roughly estimated as follows:

$$2\pi f_c \approx \left( \frac{\gamma}{\rho_1 + \rho_2} \right)^{\frac{1}{2}} \left( \frac{\pi}{2w} \right)^{\frac{3}{2}},$$

where  $\rho_1$  and  $\rho_2$  are the densities of each aqueous phase.

In the LISD measurement,  $\gamma$  was determined by independently obtaining  $w$  and  $f_c$ . The frequency response spectra of LISD for BLMs were fitted with a Lorentzian function and the corner frequency, where the signal amplitude is half of its static value at low frequencies, was determined as  $f_c$ . The spatial distribution of the laser beam,  $I$ , is given by  $I(r) = I_0 \exp\left(-\frac{2r^2}{w^2}\right)$ , where  $I_0$  is a proportional constant of a Gaussian function,  $w$  is the beam radius, and  $r$  is the distance from the beam center.<sup>17,18</sup> To evaluate  $w$  experimentally, line profiles of the acquired image of the pump beam spot reflected from the BLMs were fitted with the above function, and results from horizontal and vertical line profiles were averaged.

**Aqueous Phases on the BLMs for LISD Technique.** Radiation pressure is induced when the two media on the interfaces have different optical properties and, therefore, it was necessary to optimize the refractive indices of two aqueous phases. Dissolving the same amount of solutes with different molecular mass is one of the possible options without changing osmotic pressure on the BLM. When the molecular mass of the electrolyte dissolved in one side of the aqueous phase is different from that

of the electrolyte in the other side, BLMs are not stably formed. Hence, we used non-electrolyte solutes with different molecular mass for each aqueous phase. In a previous study, formation of vesicles using different sugar solutions (sucrose and glucose) inside and outside of the vesicles was successful.<sup>25</sup> In this study, BLMs were formed using KCl solutions containing sucrose and glucose in each aqueous phase. Large differences in the refractive index, or the density, lead to a large deformation and to fragile BLMs. In this study, a combination of two sugar solutions including 1.5 mol·L<sup>-1</sup> glucose or sucrose with 1 mol·L<sup>-1</sup> KCl and 10 mmol·L<sup>-1</sup> HEPES/KOH buffer (pH 7.4) for each aqueous phase was optimized for LISD. The densities of glucose and sucrose solutions were estimated to be 1139 g·L<sup>-1</sup> and 1232 g·L<sup>-1</sup>, respectively. In the above-mentioned conditions, the BLMs fabricated were stable for more than 1 hour and the membrane durability was enough to obtain the LISD spectrum, which was taken at room temperature.

## RESULTS AND DISCUSSION

**Validation of the Constructed LISD System.** First, we measured the 1-hexanol/water interface in the liquid/liquid system to confirm the validity of LISD. 1-Hexanol and water were added in each compartment in the PTFE chamber, which are

separated with a PTFE films with a 400- $\mu\text{m}$  diameter hole at the center and their levels were gradually and simultaneously raised over the hole. The 1-hexanol/water interface could be stably formed in the vertical configuration through the hole. Figure 3 exhibits the typical LISD spectrum obtained.  $f_c$  was estimated to be 49.6 kHz using a Lorentzian fit of the spectrum. The spot size of the pump laser was taken to be 10.5  $\mu\text{m}$  and the interfacial tension was estimated to be  $6.6 \pm 2.6 \text{ mN}\cdot\text{m}^{-1}$ . This value is in good agreement, within the margin of errors, with the  $6.45 \text{ mN}\cdot\text{m}^{-1}$  reported previously.<sup>40</sup> This result shows that the interfacial tension of the liquid/liquid interface can be determined through LISD.

**Membrane Tension of BLMs on Different Cholesterol Concentrations.** Five kinds of BLMs with cholesterol mole fractions from 0 to 33% were formed and measured. The LISD spectra are summarized in Fig. 4. In LISD spectra for BLMs with a mole fraction of more than 43%, the  $f_c$  could not be determined, because of large viscosity and changes in spectral profiles to over-damping type. The spot size was estimated to be  $7.4 \pm 0.5 \mu\text{m}$  and the membrane tension of each BLM was calculated using eq. (1). Each LISD spectrum was fitted into a Lorentzian profile and  $f_c$  was derived. The standard deviations are calculated by using triplicates. As shown in Fig. 5, the membrane tension changes between  $1.3 \mu\text{N}\cdot\text{m}^{-1}$  and  $68.1 \mu\text{N}\cdot\text{m}^{-1}$ . An increase in cholesterol in PC/PE

membranes leads to an increase of membrane tension. The membrane tension drastically increases from a 20% mole fraction of cholesterol onward, indicating that cholesterol stiffens the BLM composed of PC and PE. Further, we examined the effect of the sugar concentration in aqueous phases on the membrane tension of BLM. Typical results obtained are shown in the Electronic Supplementary Information (ESI). Increasing sugar concentration from 1.0 to 1.5 mol·L<sup>-1</sup> caused a slight decrease in membrane tension, although the effect was too small to obtain a strong correlation. The change in membrane tension caused by the addition of cholesterol in this experiment was much larger; thus, we did not have to consider the effect of the sugar concentration in aqueous phases.

The comparison with previous results has been done in the following way. There are several reported results of membrane tension of BLMs composed of phospholipids. Petelska and Figaszewski reported that the membrane tension of a pure lecithin BLM could be determined by applying a pressure difference on the sides of a convex surface and then measuring the curvature radius.<sup>38</sup> It was estimated to be 1.623 mN·m<sup>-1</sup>, and it increased to 4.715 mN·m<sup>-1</sup> when they added cholesterol, equal to the amount of phospholipid. Their values were much larger than our values. Non-invasive measurement of membrane tension of red blood cell (RBC) membranes by diffraction



phase microscopy gave results in the  $\mu\text{N}\cdot\text{m}^{-1}$  order.<sup>14</sup> Therefore, it can be considered that this large difference is due to their membrane being hardened by the pressure to the membrane, because their membranes were formed by applying pressure and deforming liquid membranes.

On the other hand, Hildenbrand and Bayerl reported that membrane tension of the BLMs composed of 1,2-dielaidoyl-*sn*-3-glycero-phosphocholine (DEPC) was  $0.42 \text{ mN}\cdot\text{m}^{-1}$  using a non-invasive method based on dynamic light scattering, and it increased to  $2.45 \text{ mN}\cdot\text{m}^{-1}$  with the addition of cholesterol.<sup>37</sup> These values were still about hundred times greater than our values. We considered two hypotheses for this massive reduction in membrane tension of BLMs. The first hypothesis is that the “solvent-free” BLM has lower membrane tension than the solvent-containing BLM.<sup>41</sup> The BLMs fabricated using the “painting” method contain more organic solvent than in the folding method and the membrane properties could be affected by it.<sup>42,43</sup> Furthermore, we carried out a LISD measurement of BLMs fabricated using the “painting” method. The egg yolk phosphatidylcholine in *n*-decane was “painted” and the membrane tension of the BLMs was estimated to be  $93 \mu\text{N}\cdot\text{m}^{-1}$ , which is also larger than that of the BLM prepared using the folding method. Therefore, the present results of the BLMs fabricated by the folding method are expected to be intrinsic values of

membrane tension without interference of organic solvents or any invasive probes.

The second considered hypothesis is that the reduction in membrane tension is due to local deformations produced by the LISD method. It was reported that BLMs had fluctuations in thickness<sup>41</sup> and viscoelasticity relaxation<sup>44</sup> and thermal fluctuations in rigidity due to a curvature effect.<sup>45</sup> The membrane tension of BLMs measured by other non-invasive methods was spatially averaged. However, in our current LISD method, the local tension of the membrane is measured at the location illuminated by the pump laser and where the membrane is deformed. The local deformation of BLMs is more sensitive to these fluctuations and relaxations, which possibly caused the reduced membrane tension.

It is known that the rigid steroid structure of cholesterol induces an orientation ordering in the adjacent hydrocarbon chains of the lipid and it decreases the surface area per molecule, which is called as the condensing effect of cholesterol.<sup>3,36,46</sup> According to the results of a Monte-Carlo simulation,<sup>47</sup> a larger condensing effect was expected when the cholesterol concentration increased. The results from dynamic light scattering<sup>48</sup> also suggest higher molar ratios of cholesterol force the lipid acyl chains to straighten, which results in a condensing effect. At molar ratios below 20%, cholesterol interacts with the polar lipid headgroups, and a slight change of membrane tension was observed. When

molar ratio increased over 20%, more ordered and rigid structures, owing to the interaction between lipid acyl chains and cholesterol, resulted in much higher membrane tension. If larger membrane tension suppresses the fluctuation of BLMs, the above results might indicate that the increase of cholesterol concentration suppress the fluctuation of BLMs.

## CONCLUSION

We have developed LISD technique for non-invasive measurement of membrane tension of the freestanding BLMs fabricated using the folding method. The obtained membrane tension of the BLM composed of PC and PE was much lower than the previous values measured by the conventional contact methods, indicating that the probe contact itself suppresses membrane fluctuation. The influence of the residual organic solvent in the BLMs could be observed by comparing the folding method with the “painting” method in BLM fabrication. The membrane tension dependence on cholesterol concentration in the BLMs composed of PC and PE was studied. It was found that the BLMs containing more than 20% cholesterol had higher membrane tension and suppressed the membrane fluctuation. The absolute value of the membrane tension evaluated by this technique is much smaller than some of those reported

previously, but the tendency is in good agreement with the previous studies qualitatively.

A combination of LISD technique and its application to the BLMs fabricated using the folding method has great potential in clarifying the correlation between the membrane function and the membrane physical properties, such as membrane tension. We are convinced that further developments will enable us to discuss on various functions and phenomena of cell membrane, such as the switching of membrane proteins and effect of nanoparticle or physiologically active substances from the viewpoint of membrane tension.

#### **ACKNOWLEDGEMENT**

This work was partially supported by JSPS (Japan Society for the Promotion of Science) KAKENHI grant No. 15H03824. The authors thank Prof. A. Hirano at Tohoku University for the great help to the formation of BLMs by the folding method.

#### **REFERENCES**

- 1 F. M. Ashcroft, *Nature*, 2006, **440**, 440.
- 2 D. Puchkov, V. Haucke, *Trends Cell Biol.*, 2013, **23**, 493.
- 3 B. Alberts, A. Johnson, J. Lewis, M. Raff, K. Roberts and P. Walter, *Molecular Biology of the Cell*, 5th ed. Taylor & Francis, New York & London, 2008.

- 4 G. Popescu, T. Ikeda, K. Goda, C. A. Best-Popescu, M. Laposata, S. Manley, R. D. Dasari, K. Badizadegan and M. S. Feld, *Phys. Rev. Lett.*, 2006, **97**, 218101.
- 5 W. Z. Helfrich, *Naturforsch.*, 1973, **28c**, 693.
- 6 P. Bassereau, B. Sorre and A. Lévy, *Adv. Colloid Interface Sci.*, 2014, **208**, 47.
- 7 G. Bao and S. Suresh, *Nature Mater.*, 2003, **2**, 715.
- 8 N. C. Gauthier, T. A. Masters and P. Sheetz, *Trends Cell Biol.*, 2012, **22**, 527.
- 9 E. Evans and W. Rawicz, *Phys. Rev. Lett.*, 1990, **64**, 2094.
- 10 D. Needham and R. S. Nunn, *Biophys. J.*, 1990, **58**, 997.
- 11 Y. Shitamichi, M. Ichikawa and Y. Kimura, *Chem. Phys. Lett.*, 2009, **479**, 274.
- 12 L. Picas, F. Rico and S. Scheuring, *Biophys. J.*, 2012, **102**, L01.
- 13 A. Aryaei and A. C. Jayasuriya, *J. Biomech.*, 2013, **46**, 1524.
- 14 Y. K. Park, C. A. Best, T. Kuriabova, M. L. Henle, M. S. Feld, A. J. Levine and G. Popescu, *Phys. Rev. E*, 2011, **83**, 051925.
- 15 E. Evans and Y. C. Fung, *Microvasc. Res.*, 1972, **4**, 335.
- 16 S. Mitani and K. Sakai, *Phys. Rev. E*, 2001, **63**, 046302.
- 17 S. Mitani and K. Sakai, *Phys. Rev. E*, 2002, **66**, 031604.
- 18 S. Mitani and K. Sakai, *Faraday Discuss.*, 2005, **129**, 141.
- 19 Y. Yoshitake, S. Mitani, K. Sakai and K. Takagi, *J. Appl. Phys.*, 2005, **97**, 024901.
- 20 Y. Yoshitake, S. Mitani and K. Sakai, *Phys. Rev. E*, 2008, **78**, 0452405.
- 21 E. Reimhult and K. Kumar, *Trends Biotech.*, 2008, **26**, 82.
- 22 H. Schönherr, J. M. Johnson, P. Lenz, C. W. Frank and S. G. Boxer, *Langmuir*, 2004, **20**, 11600.
- 23 W. Knoll, I. Köper, R. Naumann and E. K. Sinner, *Electrochim. Acta*, 2008, **53**, 6680.

- 24 T. Toyota, H. Tsuha, K. Yamada, K. Yamada, K. Takakura, K. Yasuda and T. Sugawara, *Langmuir*, 2006, **22**, 1976.
- 25 M. E. Solmaz, R. Biswas, S. Sankhagowit, J. R. Thompson, C. A. Mejia, N. Malmstadt and M. L. Povinelli, *Biomed. Opt. Express*, 2012, **3**, 2419.
- 26 M. Yanagisawa, T. Yoshida, M. Furuta, S. Nakata and M. Tokita, *Soft Matter*, 2013, **9**, 5891.
- 27 Y. Tsuji, R. Kawano, T. Osaki, K. Kamiya, N. Miki and S. Takeuchi, *Anal. Chem.*, 2013, **85**, 10913.
- 28 P. Mueller, D. O. Rudin, H. T. Tien and W. C. Wescott, *J. Phys. Chem.*, 1963, **67**, 534.
- 29 M. Montal and P. Mueller, *Proc. Nat. Acad. Sci. U.S.A.*, 1972, **69**, 3561.
- 30 A. Hirano-Iwata, M. Niwano and K. Sugawara, *Trends Anal. Chem.*, 2008, **27**, 512.
- 31 A. Hirano-Iwata, K. Aoto, A. Oshima, T. Taira, R. Yamaguchi, Y. Kimura and M. Niwano, *Langmuir*, 2010, **26**, 1949.
- 32 A. Hirano-Iwata, T. Nasu, A. Oshima, Y. Kimura and M. Niwano, *Appl. Phys. Lett.*, 2012, **101**, 023702.
- 33 A. Hirano-Iwata, A. Oshima, Y. Kimura, H. Mozumi and M. Niwano, *Anal. Sci.*, 2012, **28**, 1049.
- 34 M. Zagnoni, *Lab Chip*, 2012, **12**, 1026.
- 35 A. Ertel, A. G. Marangoni, J. Marsh, F. R. Hallett and J. M. Wood, *Biophys. J.*, 1993, **64**, 426.
- 36 P. L. Yeagle, *Biochim. Biophys. Acta*, 1985, **822**, 267.
- 37 M. F. Hildenbrand and T. M. Bayerl, *Biophys. J.*, 2005, **88**, 3360.
- 38 A. D. Petelska and Z. A. Figaszewski, *Bioelectrochem. Bioenerg.*, 1998, **46**, 199.
- 39 G. M. Hale and Query, *Appl. Opt.*, 1973, **12**, 555–563.

- 40 D. Villers and J. K. Platten, *J. Phys. Chem.*, 1988, **92**, 4023.
- 41 S. B. Hladky and D. W. Gruen, *Biophys. J.*, 1982, **38**, 251.
- 42 H. T. Tien and A. L. Diana, *Chem. Phys. Lipids*, 1968, **2**, 55.
- 43 K. V. Tabata, K. Sato, T. Ide, T. Nishizaka, A. Nakano and H. Noji, *EMBO J.*, 2009, **28**, 3279.
- 44 G. E. Crawford and J. C. Earnshaw, *Biophys. J.*, 1987, **52**, 87.
- 45 L. Peliti and S. Leibler, *Phys. Rev. Lett.*, 1985, **54**, 1690.
- 46 H. Saito and W. Shinoda, *J. Phys. Chem. B*, 2011, **115**, 15241.
- 47 F. Meyer, A. Benjamini, J. M. Rodgers, Y. Misteli and B. Smit, *J. Phys. Chem. B*, 2010, **114**, 10451.
- 48 B. A. Brüning, S. Prévost, R. Stehle, R. Steitz and P. Falus, *Biochim. Biophys. Acta*, 2014, **1838**, 2412.

Figure captions:

Figure 1 Schematic of a BLM formed on a hole with a  $\phi 400 \mu\text{m}$  hole of the PTFE film in the PTFE chamber. a. Fused silica window, b. O-ring, c. Ag/AgCl electrodes, d. PTFE chamber, e. 1.5 M sucrose aq ( $1 \text{ mol}\cdot\text{L}^{-1}$  KCl,  $10 \text{ mmol}\cdot\text{L}^{-1}$  HEPES/KOH buffer (pH7.4)), f.  $1.5 \text{ mol}\cdot\text{L}^{-1}$  glucose aq ( $1 \text{ mol}\cdot\text{L}^{-1}$  KCl,  $10 \text{ mmol}\cdot\text{L}^{-1}$  HEPES/KOH buffer (pH7.4)), g. PTFE film (thickness :  $20 \mu\text{m}$ ), h. BLM (PC, PE and cholesterol)

Figure 2 Experimental setup of LISD technique for measuring the membrane tension of BLMs.

Figure 3 LISD spectrum obtained for the 1-hexanol/water interface vertically-formed at the hole with  $\phi 400 \mu\text{m}$  of PTFE film. The solid line represents the fit using the Lorentzian function.

Figure 4 LISD spectra obtained for the BLMs composed of PC and PE with different concentrations of cholesterol, fabricated using the folding method. The solid line represents the fit using the Lorentzian function.

Figure 5 Membrane tension vs cholesterol concentration in the BLMs composed of PC and PE.



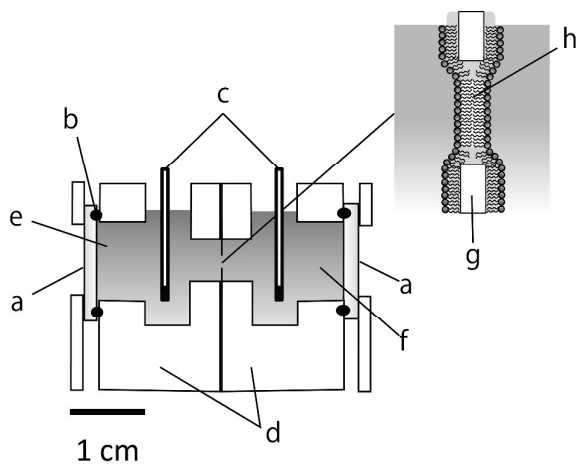


Figure 1 Schematic of a BLM formed on a hole with a  $\varnothing 400 \mu\text{m}$  hole of the PTFE film in the PTFE chamber. a. Fused silica window, b. O-ring, c. Ag/AgCl electrodes, d. PTFE chamber, e. 1.5 M sucrose aq ( $1 \text{ mol}\cdot\text{L}^{-1}$  KCl,  $10 \text{ mmol}\cdot\text{L}^{-1}$  HEPES/KOH buffer (pH7.4)), f.  $1.5 \text{ mol}\cdot\text{L}^{-1}$  glucose aq ( $1 \text{ mol}\cdot\text{L}^{-1}$  KCl,  $10 \text{ mmol}\cdot\text{L}^{-1}$  HEPES/KOH buffer (pH7.4)), g. PTFE film (thickness :  $20 \mu\text{m}$ ), h. BLM (PC, PE and cholesterol)

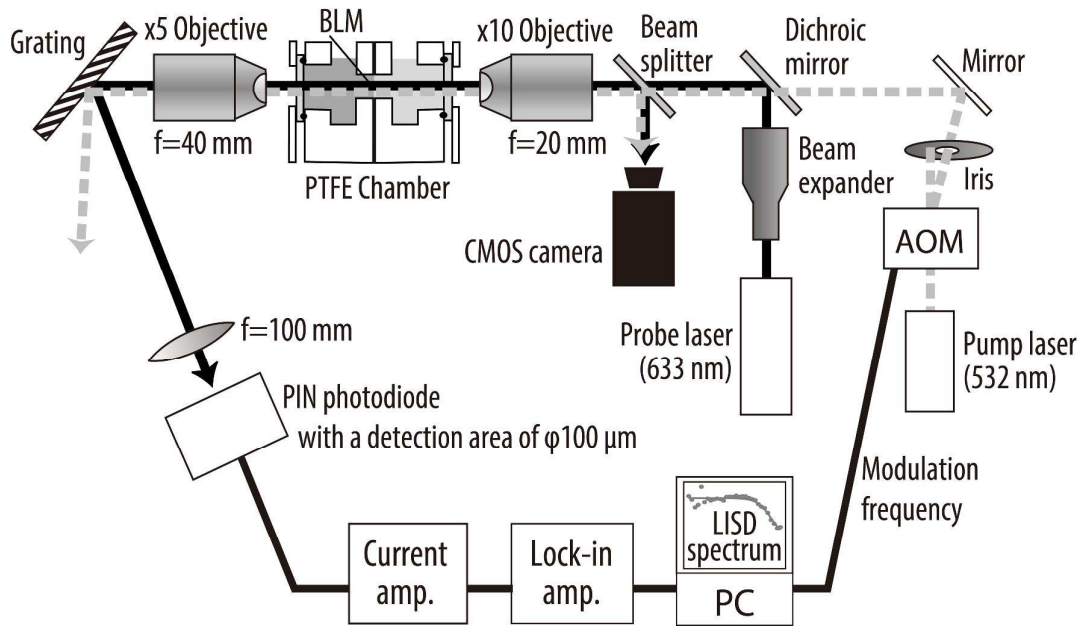


Figure 2

Experimental setup of LISP technique for measuring the membrane tension of BLMs.

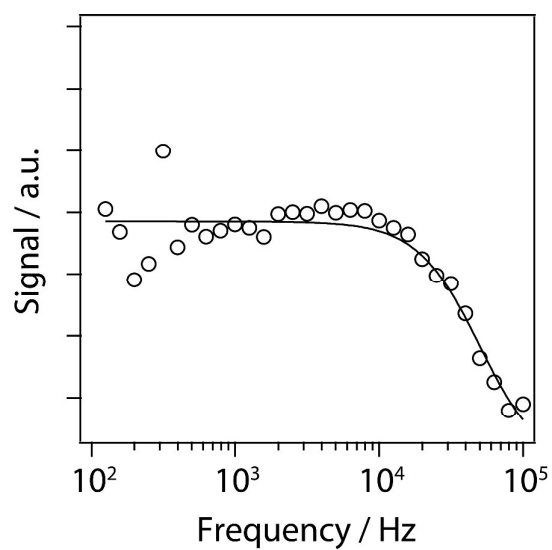


Figure 3

LISD spectrum obtained for the 1-hexanol/water interface vertically-formed at the hole with  $\varnothing 400 \mu\text{m}$  of PTFE film. The solid line represents the fit using the Lorentzian function.

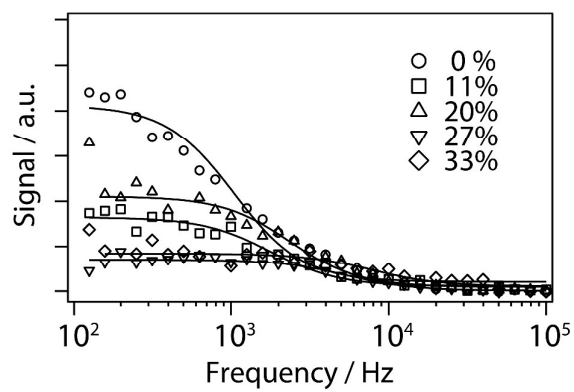


Figure 4

LISD spectra obtained for the BLMs composed of PC and PE with different concentrations of cholesterol, fabricated using the folding method. The solid line represents the fit using the Lorentzian function.

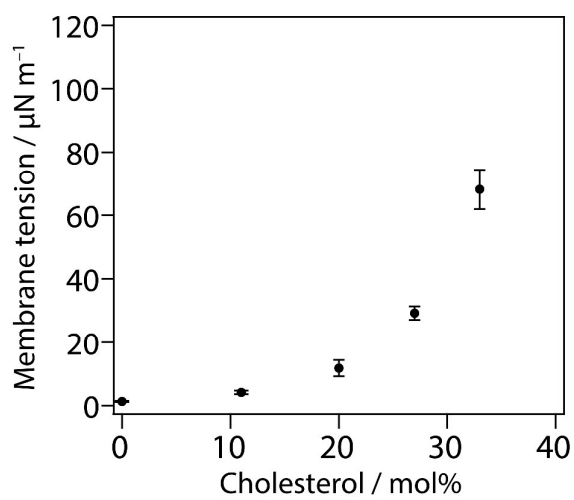


Figure 5

Membrane tension vs cholesterol concentration in the BLMs composed of PC and PE.

For TOC only

